1D models for thermal and air quality prediction in underground traffic systems

Per Sahlin, Lars Eriksson, Pavel Grozman, Hans Johnsson and Lars Ålenius
Equa Simulation AB, Sweden

ABSTRACT

Long-term prediction of thermal and air quality parameters in complex underground metro systems presents a significant challenge. Established simulation tools are available but dated and several important aspects are inadequately treated. The recent Hybrid DAE modelling language Modelica and associated simulation environments represent an opportunity to more efficiently develop, manage and solve complex multi-domain models. The method has rapidly gained momentum within several industries such as automotive, aerospace and electronic. A new Modelica based tunnel simulation environment has been developed, validated and tested by external users in the context of several full scale projects. Some salient novel features are:

- The long-term temperature profile into the tunnel wall under the influence of radial water seepage is computed without any radical assumptions or simplifications. Interaction with ground surface and neighbouring tunnel temperature fields are treated.
- Long-term schedules and measured climate data enable correct prediction of the interaction of piston, buoyancy and meteorological forces.
- In addition to hygrothermal, the following air properties are computed: age, i.e. total time spent under ground; carbon dioxide, mostly generated by occupants; particle concentration, e.g. PM10 as generated by train movements; optical extinction coefficient from fire and diesel smoke; CO, NO_x and HC, as generated by diesel powered vehicles.
- Both rail and road traffic may be modelled. For road traffic, a continuous flow model capable of describing realistic congestion scenarios is available.
- A library of HVAC equipment, fans, dampers, Saccardo nozzles and similar components is available, enabling both transversal and longitudinal ventilation studies.
- A library of continuous control components such as sensors, PID-controllers, filters, switches etc. enables detailed off-line control design.
- A 3D tunnel editor is available for input data checking and visualization of results.
- Ice and mould (mildew) build-up may be computed.

Initial validation studies have been performed with respect to other 1D programs, CFD, analytical solutions, fire experiments and underground system measurements.

1 INTRODUCTION

Ensuring an adequate indoor environment in underground facilities is often a difficult engineering task. It is not always obvious which air property becomes most critical. Several physical phenomena interact with timescales that may vary by many orders of magnitude. In underground metro systems, ventilation and heat balance is given by a complex interaction of for example: train piston action and heat emission; buoyancy driven flow; wind induced and meteorological pressure differences on portals and openings and by mechanical HVAC systems. Train scheduling and control strategies for non-HVAC components such as doors may also have a profound impact on indoor climate and long term thermal response. In the field, it is easy to find examples of expensive service systems that, after some years of operation, have never been put to use as originally intended or have proven to be insufficiently sized.

The degree of authority of mechanical HVAC systems varies greatly between different subways. Early facilities were designed with primitive engineering methods but may nevertheless have acceptable climate without mechanical ventilation while traffic loads remain modest. However, with increasing traffic, mechanical measures must sometimes be retrofitted to remove excessive heat both from present and, by cooling the surrounding ground, past operation. More recent subways may have high-capacity HVAC systems that maintain good conditions but at great expense both in terms of installation and energy cost. In an increasingly energy conscious society, it may be important to secure predictable underground climate based primarily on passive measures and smart control while minimizing the need for heavy HVAC equipment. Being able to reliably predict by a virtual model the long-term behaviour of the total physical system becomes essential for finding economical and ecological solutions.

The ambitious development of the Subway Environment Simulation (SES) program in the early seventies (1) represented a giant step forward for an engineer's ability to predict aerodynamic and thermal phenomena and to size mechanical systems. Consequently, the design of most modern subways has greatly benefited from SES ventilation design computations.

Two main arguments made us consider the development of a new tool in the SES tradition. Firstly, for the projects at hand, some important physical effects were not modelled in SES. Secondly, recent advances in both software and hardware make it possible to create a more modern engineering tool with substantially improved usability and flexibility.

Some areas that are inadequately treated in SES v. 4.1 are:

- Heat sink effect. SES offers an estimate of long-term ground heat storage based on a drastic extrapolation of system state. Time dependent variations in system operation are not adequately treated.
- Buoyancy driven flow is not treated for line sections, except for fire cases.
- Feedback control. It is not generally possible to study system operation based on measured system state.
- Computation of other air properties in addition to temperature and humidity. For many design situations, other air quality measures or smoke propagation are the primary focus.

Study of comfort issues due to interacting travelling pressure-waves is another area where the incompressible problem formulation of SES becomes inadequate. For many modern high speed train tunnels, pressure discomfort is a key design issue. Also in subways with a high blockage ratio, pressure discomfort may occur. However, in this respect, we have made a similar reflection as must have been made during the development of SES: spending computational effort on resolving this high-frequency phenomena is not economical for the longer term studies that are of concern here. In spite of today's awesome processing power, long-term and large-scale subway simulation still involves significant execution times, leaving room only for computation of effects that are of primary interest.

In addition, pressure wave studies normally require exceptional traffic scenarios that need special attention both in terms of input and output. Obviously, it is practical to be able to reuse train and tunnel physical parameters for this type of study, but repeated computation of this effect for thousands of train passages is, in our opinion, unlikely to ever become desirable.

A commonly adopted approach for thermal computations of rail tunnel systems is to first, as a pre-processing step, compute train induced air movements, for example using a compressible tool such as THERMOTUN (2). Then to import resulting air flows into a separate tool, for subsequent computation of heat, moisture and possibly other advected air properties. This way, only a single cycle of train operation needs to be computed and this is then replayed numerous times to reach the thermal time scales. In such a scenario, the resolution of pressure waves in the air movement computation represents a marginal extra cost and undesirable high-frequencies may even be filtered out before import into the thermal post-processing. However, this type of two-step operation precludes the possibility of easily studying feedback effects between the thermal results and system air flows. The most obvious such effect is that of thermal buoyancy, but equally important may also be feedback control loops, that affect, e.g., fan or damper operation in response to measured system signals.

Another aspect of using pre-recorded air flows relates to the nature of the train piston effect. Train synchronisation becomes highly influential on net transport effects, and consequentially, study of statistical variations in train scheduling becomes crucial. Irregular train scheduling due to statistical effects reduces the potential savings that may be achieved by pre-computation of air flows. (A repeatable train cycle becomes very long, if it exists at all.) A similar argument can be made about seasonal variations in shaft and door opening schedules.

Let us now turn to the second main motivation for the new development. Large and complex Fortran programs from the early days of engineering computing exist in almost every domain. After countless rounds of improvements and extensions, they tend to become quite unmanageable – even for the original developers. Simulation researchers have therefore tried to invent systematic ways of describing large-scale physical systems with radically improved scalability and flexibility in comparison with tailored codes but with no or marginal sacrifice of numerical efficiency. Since countless smart, insight driven, efficiency measures have been implemented in the domain specific codes, reaching adequate numerical efficiency has often proven to be the stumbling block. However, recently a technology based on system descriptions in terms of symbolic differential-algebraic systems of equations (DAE) has shown unparalleled success. Not only is it possible to recreate many legacy codes with a fraction of the development effort, and in many cases improved performance, but due to the generality of the approach much larger multi-domain models, including controllers, may be efficiently managed and operated.

In the automotive industry, there is generally a large code for each main system of a car: engine, drive-line, braking, multi-body motion etc. Numerous less successful attempts at co-simulation with several simultaneous executables, made automotive engineers attempt to re-model everything in the new DAE based language Modelica (www.modelica.org). The change of technology proved a success (3) and Modelica is now a de facto standard for large-scale lumped parameter modelling not only in automotive but also in several other industrial sectors.

Rather than starting from the technical details, we will in the next section present some examples of applications of the new tool: IDA Tunnel. After that, a selection of implemented physical effects and models are presented with some validation studies in Section 3, followed by a brief discussion of the implementation methods. Remaining issues are discussed and conclusions are drawn in Sections 5 and 6.

2 APPLICATION EXAMPLES

2.1 Simple double track tunnel

We will start with an artificial example, to get a feeling for the relative importance of some of the physical effects that influence the heat balance of a tunnel. We will assume the following:

- A 1000 m long 40 m^2 tunnel.
- 5 minute traffic in both directions (12 m^2 front area, 72 km/h). Train parameters have been selected so that no heat is emitted from the train. Train bodies do not store heat in the example. Only friction heat is generated by the traffic (amounting to approx. 104 kW). No trains run between 01:00 and 05:00, otherwise traffic is constant.
- Artificial (convective) train heat is emitted separately at 500 W/m during the hours of train operation (to avoid variability in heat emission).
- Initial temperature is 0˚C and ambient temperature is kept constant at 0˚C. No moisture is considered.

We will consider three cases without wall heat storage and one with a rock wall:

1. Adiabatic tunnel wall, no inclination, train traffic staggered by 150 s, i.e. trains from one side enter exactly halfway between those from the other.
2. Same as 1, except trains are staggered by 75 s, creating an asymmetric traffic rhythm.
3. Same as 1, except tunnel has 10 m inclination.
4. Same as 3, except with an infinite rock wall.

Four result variables during train operation are reported: Net heat emitted from each tunnel portal, the maximum air temperature inside the tunnel and the maximum age of tunnel air, i.e. how long the oldest air in the tunnel has been under ground. Table 1 shows results.

Table 1. Results for Case 1-3

case	left Q [kW]	right Q [kW]	tmax ˚C	age [h]
1.	302	302	8.4	0.208
2.	89	515	8.0	0.164
3.	83	522	7.6	0.158

The asymmetric traffic rhythm (in a level tunnel) leads to a slightly lower maximum temperature and, somewhat surprisingly, to a substantially increased level of ventilation (27%). As can be expected, the most dramatic effect is in the distribution of train heat out of the tunnel, where only 15% of the heat is emitted from the left portal. In Case 3, where the traffic is symmetric again, we note a similar but even more pronounced change in the same variables. Disregarding the effect of buoyancy does not seem to be appropriate, even with this rather modest tunnel inclination.

Before leaving this artificial example, let us also take a brief look at dynamic effects. Case 4 is the same inclined tunnel with symmetric traffic as in Case 3, but now with an infinite rock wall. Figure 1 shows hourly averages of the portal heat fluxes during the 30 first days of operation. Buoyancy leads to a significant heat emission at night out of the higher (right) portal. In a tunnel with no or limited train traffic, this will be the dominant heat transfer mechanism.

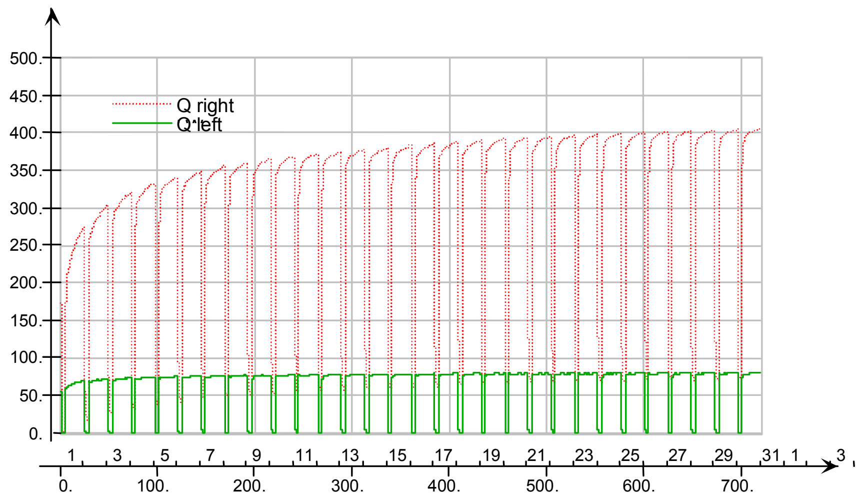

Figure 1. Case 4 for 30 days.

During day 30, the average heatflux out of the right portal is 346 kW to be compared with the daily average of Case 3 of 433 kW. After a month, 87 kW is still absorbed by the wall. Case 4 was also simulated for 30 years of operation and after this period the corresponding figure was 21 kW. The rock is then heated by 5.3 ˚C at the surface and 0.5˚C approximately 50 m into the wall, storing in total some 33 GWh. This heat represents a non-negligible cost if it were cooled away by mechanical means.

Now we will very briefly present some full-scale models done in IDA Tunnel. Due to space constraints only a small sample of computational results will be included.

2.2 Stockholm Metro

Like many other metro operators, Stockholm Transport (SL) are concerned with high particle levels in the underground environment. The above-ground European norm of 50 µg/m3 pm10 (mass of particles which are 10 µm or smaller) is exceeded in some stations by an order of magnitude. In other subways around the world, the situation is even worse, with levels better measured in milligrams. Any hope of limited health effects of subway dust also seems overly optimistic, with recent studies showing in-vitro genotoxic effects (4).

For reasons previously discussed, and since the primary focus was on air quality rather than on thermal effects, it was decided to develop a new Modelica based rail tunnel simulator, using SES primarily as a source of knowledge and point of reference.

The first model developed with the new tool was of the section between Slussen and Liljeholmen stations in Stockholm (Figure 2). Platforms here are modelled as well-stirred volumes. It is also possible in IDA Tunnel to use tunnel segments for modelling platforms.

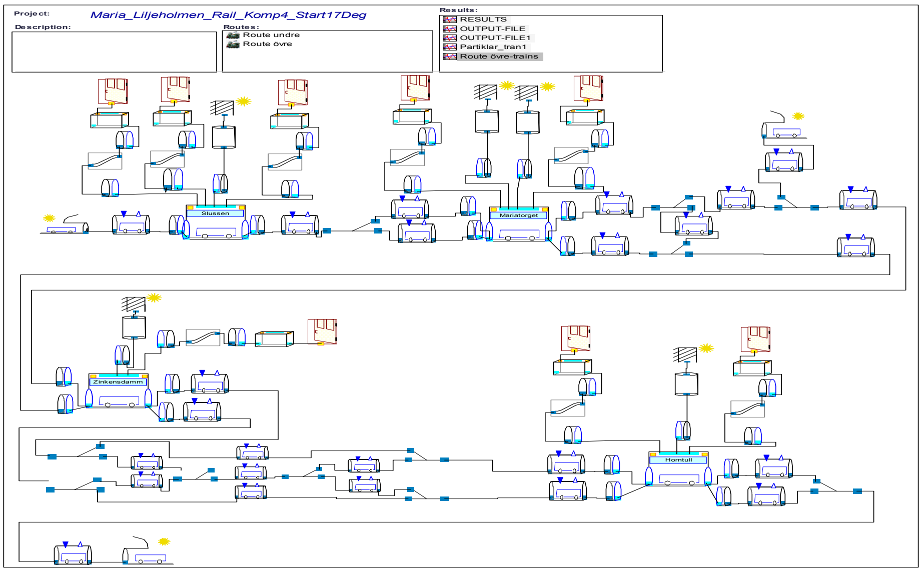

Figure 2. The schematic representation of tunnels, platforms, shafts, and openings of the Slussen-Liljeholmen section.

A simple model for train particle emissions has been developed assuming source terms proportional to rolling resistance and mechanical braking. The source terms have then – lacking more fundamental understanding of the emission mechanism – been calibrated against measurements. Figure 3 shows a comparison between particle level measurements and simulation results. Absolute levels are reasonably correct due to the calibration procedure. The diurnal variations are also in acceptable agreement with measurements. It should be emphasized that the particle generation mechanisms through mechanical wear are not yet fully understood and further multi-disciplinary work is needed.

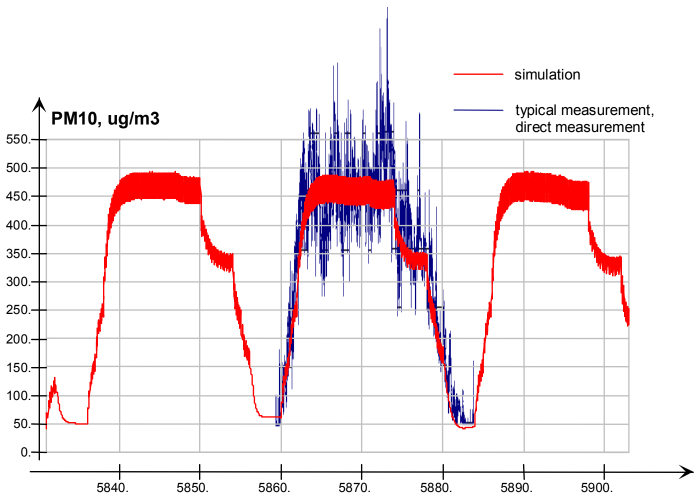

Figure 3. Computed diurnal variation in particle levels on the subway platform at Mariatorget in Stockholm. The second day shows also a measured sequence.

Similar models have also been developed for the other underground sections of the Stockholm metro.

2.3 Citybanan tunnel in Stockholm

A new 6.5 km commuter rail tunnel under Stockholm is planned for opening in 2013. Two stations interconnect the new tunnel with three existing subway lines. Trains will be running with a maximum speed of 80 km/h through 70 m^2 double track tunnels.

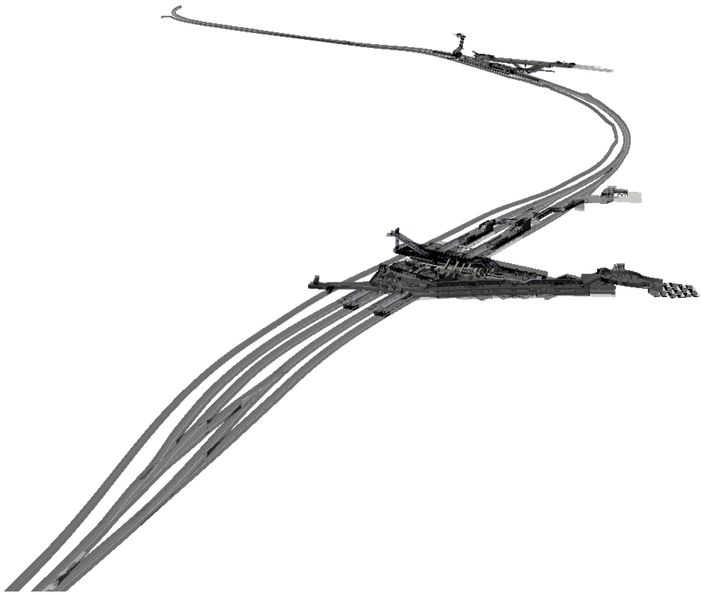

Figure 4. An image from the 3D environment of IDA Tunnel of the Citybanan model. Along the stretch of the rail line runs a service tunnel.

Due to city planning constraints, the number of ventilation shafts is to be kept at a minimum and the deep, spacious tunnels with two-way traffic lead to rather limited “free” ventilation due to piston action. Without mechanical ventilation measures, the stations would overheat, particle levels would be unacceptable and the age of air would exceed five hours during summer (but be considerably lower during winter due to buoyancy driven flow). At the time of writing, the suggested ventilation system runs 30 m^3/s of supply air from both portals of the service tunnel to each station. The annual heat storage in the service tunnel wall will in this way provide in excess of 1 MW of free cooling in the summer and similar heating in the winter. (The design outdoor temperature is –18˚C.) Exhaust air from stations is to be conveyed with jet fans in the single track train tunnels to portals and a single exhaust shaft between the stations. Fans are controlled by velocity feedback in order to maintain desired average tunnel flows against the contaminant gradients. Figure 5 shows particle levels along a path through the system during peak particle conditions. Electrostatic filters on stations are considered as an additional measure for further reducing particle levels (not applied in the example).

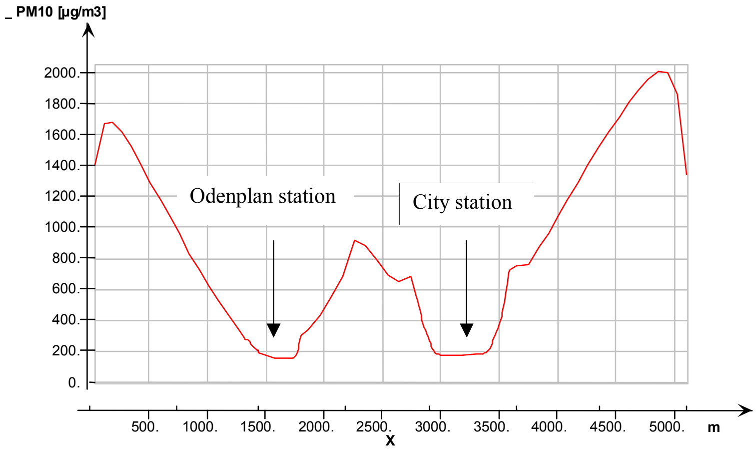

Figure 5. Computed PM10 particle levels in Citybanan.

Extensive fire studies have been performed in the scope of the Citybanan project. 1D models have then been used to determine bulk airflows and temperatures as a function of time. Figure 6 shows an example of a 1D study of smoke propagation in an escalator shaft at City station as animated in the 3D visualization environment of IDA Tunnel. For critical fire evacuation situations 1D results have also provided boundary conditions for detailed CFD studies.

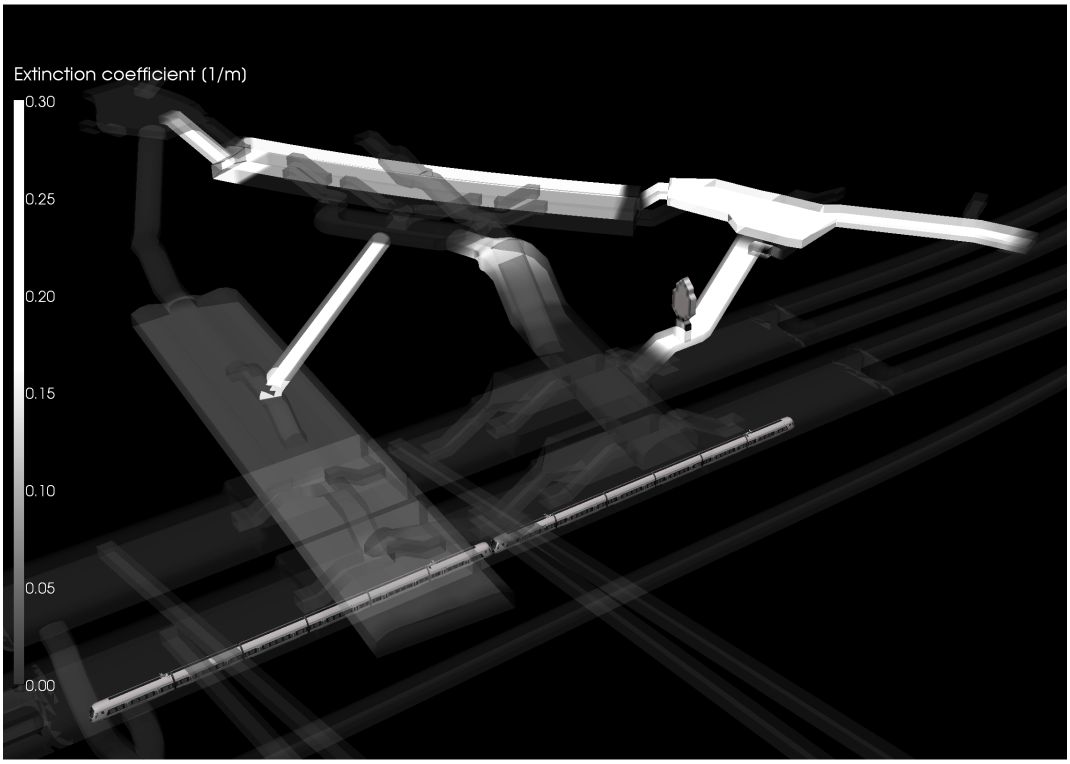

Figure 6. A snapshot of a 1D smoke and train animation

3 MODELS AND VALIDATION EXAMPLES

The system models of the Stockholm metro have since 2002 been favourably compared with velocity, pressure and temperature measurements. However, full-scale system models contain such a high proportion of estimated parameters that they are of limited value for program diagnostics. Comparisons with established simulation models are another way to validate a new model. A selection of such studies that have been carried out will be presented here.

3.1 Vehicle tunnel aerodynamics

The train aerodynamic parameters of IDA Tunnel have been selected to correspond to those of SES. Let us dive into some details and look at some of the main contributing terms of the aerodynamic equations. Equations (1), (2), (3) and (4) below give the basic pressure contributions from friction, train piston action and buoyancy.

$$\Delta p_{frict} = -\sum_i \frac{\rho_i}{2}\frac{\lambda_T}{d_i}[(l_i - \sum_j l_{V\_ij})v_i|v_i| - \sum_j \frac{l_{V\_ij}}{(1-A_{V\_j}/A_i)^3}(\frac{A_{V\_j}}{A_i}v_{V\_ij} - v_i)\left|\frac{A_{V\_j}}{A_i}v_{V\_ij} - v_i\right|] \quad (1)$$

where

Δp_{frict}	=	pressure change due to friction against walls (Pa)
λ_T	=	friction factor for tunnel wall
ρ_i	=	mean density of air in tunnel segment i (kg/m^3)
d_i	=	hydraulic diameter of tunnel segment i (m)
l_i	=	length of tunnel segment i (m)
l_{V_ij}	=	length of vehicles of type j in tunnel segment i (m)
v_i	=	mean air velocity in segment i, positive from left to right (m/s)
v_{V_ij}	=	velocity for vehicle j in segment i, positive from left to right (m/s)
$A_{V\,j}$	=	cross section area of vehicle type j (m^2)
A_i	=	tunnel area of segment i (m^2)

$$\Delta p_{fricv} = \sum_i \sum_j \frac{\rho_i}{8}\frac{\lambda_{V\_j}\cdot l_{V\_ij}\cdot p_{V\_j}}{A_i(1-A_{V\_j}/A_i)^3}(v_{V\_ij} - v_i)|v_{V\_ij} - v_i| \quad (2)$$

where $\lambda_{V\_j} = \lambda_{VS\_j} + \dfrac{c_{DTV\_j}}{4 l_{V\_j} p_{V\_j}}$

Δp_{fricv}	=	pressure change due to friction against vehicles (Pa)
$\lambda_{V\,j}$	=	skin friction coefficient for vehicles of type j
$\lambda_{VS\,j}$	=	skin friction coefficient related to viscous drag for vehicles of type j
$c_{DTV\,j}$	=	drag coefficient weighted total truck area of vehicle type j (m^2)
$l_{V\,j}$	=	length of vehicles of type j (m)
$p_{V\,j}$	=	perimeter of vehicles of type j (m)

$$\Delta p_{piston} = \sum_i \sum_j \frac{\rho_i}{2}A_{V\_j}\{[\frac{c_{DFV\_j}}{A_i} + \frac{(2A_i - A_{V\_j})}{(A_i - A_{V\_j})^2}]N_{front\_ij} + [c_{DBV\_j}\frac{A_i}{(A_i - A_{V\_j})^2} - \frac{2}{A_i - A_{V\_j}}]N_{back\_ij}\}(v_{V\_ij} - v_i)|v_{V\_ij} - v_i| \quad (3)$$

where $c_{DBV\_j} = \dfrac{0.029}{\sqrt{0.5\lambda_{VS\_j} l_{V\_j} p_{V\_j}/(4A_{V\_j})}}$

Δp_{piston}	=	piston pressure rise (Pa)

c_{DBV_j} = drag coefficient at back end of vehicle type *j*
c_{DFV_j} = drag coefficient at front end of vehicle type *j*
N_{front_ij} = # of front ends (see below) of vehicle type *j* in segment *i*
N_{back_ij} = # of back ends (see below) of vehicle type *j* in segment *i*
Front end is here defined as the end, either physical front or back, which has headwind.

$$\Delta p_{stack} = -\sum_i \rho_i \cdot \Delta h_i \cdot g \quad (4)$$

Δp_{stack} = stack pressure rise (Pa)
Δh_i = change of altitude in segment *i* (m)
g = 9.80665 = acceleration of gravity (m/s^2)

Naturally, a number of comparisons have been made to confirm the replication of SES aerodynamic results. Due to substantial differences in discretisation and solution schemes, exact reproduction of SES results cannot be expected. Table 2 gives an example of air flow in a 2 km, 20 m^2 tunnel, with single direction 5 minute traffic of 10 m^2 trains at 72 km/h.

Table 2: Summary of flow results from SES and IDA

	SES Fric fac 0.065	IDA Fric fac 0.065	SES Fric fac 0.093	IDA Fric fac 0.093
Max volumeflow [m^3/s]	128.8	130.3	123.0	120.8
Min volumeflow [m^3/s]	13.8	13.1	9.99	9.55
Average volumeflow [m^3/s]	64.8	63.7	59.1	56.6
Max air velocity [m/s]	6.44	6.50	6.15	6.04
Min air velocity [m/s]	0.69	0.66	0.50	0.48

To compare the incompressible solution of IDA Tunnel with a well-tested compressible rail aerodynamic tool, a version of the full Citybanan model was converted into the format of THERMOTUN (2). Figure 7 shows aperture air velocities at the Odenplan station as computed by THERMOTUN after a single 80 km/h train passage. Fast oscillations due to multiple reflections of pressure waves can be observed.

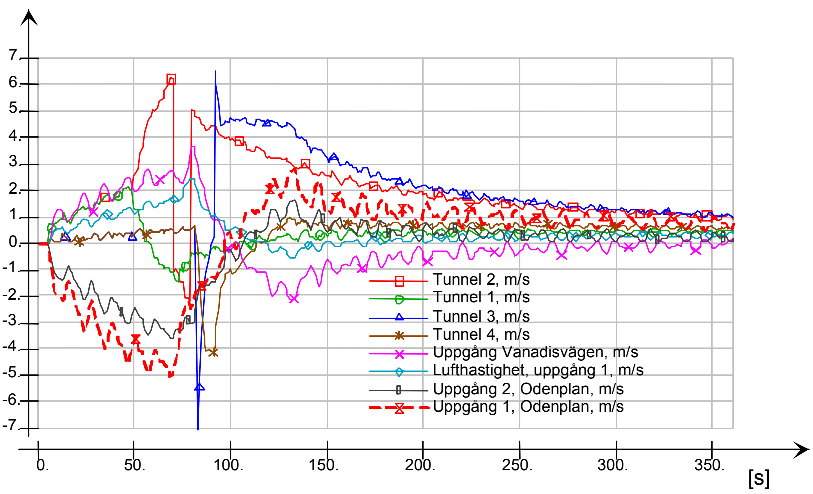

Figure 7. Aperture air velocities as computed by THERMOTUN

The corresponding flow pattern from IDA Tunnel, shown in Figure 8, is obtained with about two orders of magnitude less computational effort. The oscillations due to inter reflecting waves are not reproduced, but bulk airflows correspond well. Only bulk airflows will contribute to ventilation characteristics.

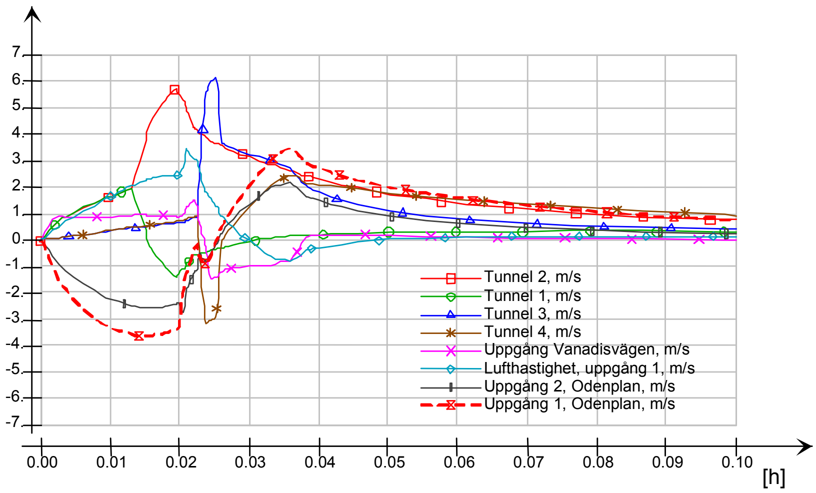

Figure 8. Air velocities computed by IDA Tunnel

3.2 Wall temperature profile

The temperature field into the surrounding ground caused by conditions in the section/platform is computed using the one-dimensional conduction-advection equation in cylindrical coordinates. This is done around each segment in sections and around each platform. The thermal properties are allowed to vary radially by using layers with different properties. The full implementation also computes a vertical temperature field in the surrounding ground and contributions from this and from neighbouring tunnels are superimposed with the solution from the current tunnel. This superposition process is not covered here due to space constraints.

$$2\pi r \rho_{wall}(r) c_{pWall}(r) \frac{\partial T_r}{\partial t} = 2\pi \frac{\partial}{\partial r}(k_{wall}(r) r \frac{\partial T_r}{\partial r}) + m_{seep} c_{pWat} \frac{\partial T_r}{\partial r} \quad (5)$$

with boundary conditions

$$2\pi k_{wall}(r_0) r_0 \frac{\partial T_r}{\partial r} = \alpha (T_{air} - T_{wall}) + Q_{wall} / l \quad \text{at wall surface } r_0$$

$$\frac{\partial T_r}{\partial r} = 0 \quad \text{or} \quad T_r = 0 \qquad \text{at outer boundary of computational domain}$$

where

T_r	= temperature change in wall caused by conditions in segment/platform/plenum (˚C)
T_{wall}	= temperature of wall surface (˚C)
$\rho_{wall}(r)$	= density in wall (kg/m^3)
$c_{pWall}(r)$	= specific heat in wall (J/kg˚C)
c_{pWat}	= specific heat of water (J/kg˚C)
m_{seep}	= water seepage/meter out of wall (kg/sm)
$k_{wall}(r)$	= thermal conductivity in wall (W/m˚C)
α	= $U \cdot A_{wall} / l$ = heat transfer coefficient between wall and

segment/platform/plenum (W/m˚C)

U = total heat transfer coefficient containing convection and radiation depending on temperature, extinction coefficient and hydraulic diameter (see 2.2.1-3) (W/ m^2˚C)

A_{wall} = wall area of segment/platform/plenum (m^2)

l = length of segment/platform/plenum (m)

r_0 = half the hydraulic diameter (m)

T_{air} = air temperature in segment/platform/plenum (˚C)

T_∞ = undisturbed wall temperature (˚C)

The heat transfer coefficient U depends on radiation and convection

$$U = U_{rad} + U_{conv}$$

with

$$U_{rad} = em_{gas} \cdot \sigma \cdot (K_{air}^2 + K_{wall}^2) \cdot (K_{air} + K_{wall})$$

and

$$U_{conv} = k_1 \cdot \max(h, U_{film})$$

where

h = $Nu \cdot k_{air} / d$ = convective heat transfer coefficient (W/ m^2˚C)

U_{film} = heat transfer coefficient at low air velocities computed as a function of the temperature difference between air and wall. From IDA Indoor Climate and Energy 3.0 (W/ m^2˚C)

k_1 = factor (e.g. for surface enlargement)

Nu = $(\lambda_T/8) \cdot (Re - 1000) \cdot Pr / (1 + 12.7 \cdot \sqrt{(\lambda_T/8)} \cdot (Pr^{2/3} - 1)) =$ Nusselt number (6)

Re = $|v_{air}| \cdot \rho_{air} \cdot d / \mu_{air}$ = Reynolds number

Pr = $c_{pAir} \cdot \mu_{air} / k_{air}$ = Prandtl number

λ_T = friction factor for tunnel wall

c_{pAir} = specific heat of air (J/kg˚C)

$k_{air}(T)$ = thermal conductivity in air. Approximated by a 3-degree polynomial in T_{air} fitted to table data in (6) (W/ m˚C)

$\mu_{air}(T)$ = dynamic viscosity in air. Approximated by a 3-degree polynomial in T_{air} fitted to table data in (6) (Pa s)

K_{air} = $(T_{air} + 273.15)$ = absolute temperature of air (K)

K_{wall} = absolute temperature of wall (K)

em_{gas} = $1 - e^{-ext \cdot d}$ = gas emission

ext = extinction coefficient (m^{-1})

σ = $5.6697 \cdot 10^{-8}$ = constant of Stefan-Boltzmann (W/ m^{2}K^4)

d = hydraulic diameter (m)

v_{air} = air velocity (m/s).

The solid line in Figure 9 shows an example of an exact solution of Equation (5) (m_{seep}=0) after 12 years in response to a 20˚C step temperature change on the wall surface. Material parameters are: ρ = 2700 (kg/m^3), c_p = 880 (J/kg°C), k = 3 (W/m°C), i.e. rather typical rock properties.

Ten cells into the wall have been computed in the corresponding IDA Tunnel case, with two different grid factors:'+' grid factor =1, 'x' grid factor=1.5. (The latter is default.)

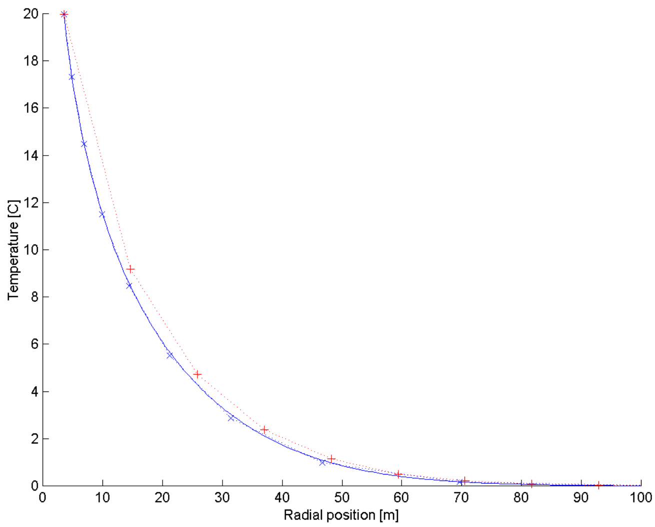

Figure 9. Computed temperature profiles in wall.

4 IMPLEMENTATION METHOD

As previously mentioned, the mathematical models of IDA Tunnel have been implemented in the Modelica language. IDA Simulation Environment (5) has been the Modelica platform used and the user interface toolkit offered by IDA SE has been fully utilized. Modelica is a language for specifying simulation models in terms of so-called Hybrid DAEs, i.e. differential-algebraic equations with discrete events and hysteresis. The primary advantage for the developer (and user) is that model equations are stated without any concern as to how they are to be solved. This makes the model code comparatively simple and succinct. The actual solution is computed by a combination of symbolic and numerical methods of the Modelica environment used. A tolerance parameter determines how accurately to solve equations, and by decreasing this it is always possible to solve equations to an arbitrary order of accuracy and thereby eliminate solution errors. Below is an example of the Modelica source code for the Saccardo nozzle component. An advanced user may change the standard models of IDA Tunnel or add his/her own using IDA Simulation Environment.

```
model SaccarNoz
  "Saccardo nozzle; bi-dir air w fractions"

    outer parameter ArraySize nFract;

    parameter Area aTun1(min=0.0)=75.0          "cross section area 1";
    parameter Area aTun2(min=0.0)=75.0          "cross section area 2";
    parameter Area aTun3(min=0.0)=75.0          "cross section area 3";
    final
    parameter Area aTun12=(aTun1+aTun2)/2       "mean of area 1 and 2";
    parameter Real Kmx=0.8                      "Momentum exchange coefficient";
    parameter Real Fi(min=0.0, max=180.0)=15.0 "Angle between nozzle 3 and tunnel 1";
    parameter Pressure PAmb(min=0.0)=101325.0  "ambient pressure at reference level";
  protected // Calculated parameters
    parameter Real cosFi                        "cos(Fi)";
  public // Variables
    Density Rho1(min=0.5, max=3.0, start=1.2)  "density of tunnel air 1";
    Density Rho2(min=0.5, max=3.0, start=1.2)  "density of tunnel air 2";
    Density Rho3(min=0.5, max=3.0, start=1.2)  "density of tunnel air 3";
    Temp_C T(min=Const.T_zero, start=20.0)     "Temperature out of node";
    flow Velocity VAir1(start=0.0)             "air speed tunnel 1";
    flow Velocity VAir2(start=0.0)             "air speed tunnel 2";
    flow Velocity VAir3(start=0.0)             "air speed nozzle 3";
```

```
    flow VolumeFlowRate
       VFAir1(start=0.0)                        "air volume flow 1",
       VFAir2(start=0.0)                        "air volume flow 2",
       VFAir3(start=0.0)                        "air volume flow 3";
    Real[nFract] vf                             "fractions out of node",
                 vf1                            "fractions at 1",
                 vf2                            "fractions at 2",
                 vf3                            "fractions at 3";
    Pressure PT1(start=1.0)                     "terminal 1 total pressure";
    Pressure PT2(start=2.0)                     "terminal 2 total pressure";
    Pressure PT3(start=0.0)                     "terminal 3 total pressure";
/*
    Real dir1(start=1) = noEvent(sign(tun1.m_dot));
    Real dir2(start=1) = noEvent(sign(tun2.m_dot));
    Real dir3(start=1) = noEvent(sign(tun3.m_dot));
*/
  // Connectors
    TunnelCut tun1(T=T, vf=vf),
              tun2(T=T, vf=vf),
              tun3(T=T, vf=vf);


  // Equations
  equation
    // Parameter Processing
    cosFi = Math.cos(Fi*Const.PI/180);

    Rho1 = (PAmb+tun1.P)/GASCON/(T-Const.T_zero);
    Rho2 = (PAmb+tun2.P)/GASCON/(T-Const.T_zero);
    Rho3 = (PAmb+tun3.P)/GASCON/(T-Const.T_zero);

    VFAir1 = tun1.m_dot/Rho1;
    VFAir2 = tun2.m_dot/Rho2;
    VFAir3 = tun3.m_dot/Rho3;

    VAir1 = VFAir1/aTun12;
    VAir2 = VFAir2/aTun12;
    VAir3 = VFAir3/aTun3;

    PT1 = tun1.P + Rho1/2*VAir1^2;
    PT2 = tun2.P + Rho2/2*VAir2^2;
    PT3 = tun3.P + Rho3/2*VAir3^2;

/* Continuity equations */
    0 = tun1.m_dot + tun2.m_dot + tun3.m_dot;
    0 = tun1.Q + tun2.Q + tun3.Q;
    zeros(nFract) = tun1.vf_dot + tun2.vf_dot + tun3.vf_dot;

    tun3.P = tun1.P;

/* Momentum equation */
    (tun1.P - tun2.P)*aTun12 = tun2.m_dot*VAir2 - tun1.m_dot*VAir1 - tun3.m_dot*VAir3*cosFi*Kmx;

    vf1 =  (if noEvent(abs(VFAir1) < 1.0E-4) then zeros(nFract) else tun1.vf_dot/VFAir1) ;
    vf2 =  (if noEvent(abs(VFAir2) < 1.0E-4) then zeros(nFract) else tun2.vf_dot/VFAir2) ;
    vf3 =  (if noEvent(abs(VFAir3) < 1.0E-4) then zeros(nFract) else tun3.vf_dot/VFAir3) ;


  // Problem
  annotation(
    IDA(
      Input  = {tun3.vf_dot, tun1.vf_dot, vf, tun3.Q, T, tun3.m_dot, tun1.m_dot, tun3.Q, tun1.Q, tun2.P},
      Output = {tun2.vf_dot, tun2.m_dot, tun2.Q, tun3.P, tun1.P},
      Role = SaccarNoz
  ));

end SaccarNoz;
```

The example above contains only algebraic equations, but ordinary differential equations may also be directly stated. Partial differential equations must be “manually” discretised in space. The spatial resolution will then typically be controlled by a user-defined parameter, i.e. this discretisation inaccuracy is not managed by any global tolerance parameter.

5 FURTHER WORK

IDA Tunnel has been used on real-scale projects since 2003 but is nevertheless in the very early stages of its life cycle. It is expected that encounters with larger circles of users and new project challenges will lead to many improvements and extensions in the near future.

Some areas where in-house development is underway are:

- Further validation studies, both with respect to other models in 1D and 3D and to full-scale measurements. Tracer gas measurements are planned to validate basic transport properties.
- Improvement of models of branch (junction) total pressure losses. IDA Tunnel contains implementations of analytical correlations from Gardel (7) and SES, but both of these

have problems. Gardel only covers a limited number of tunnel geometries, while SES correlations contain discontinuities that are unphysical and that may cause numerical instabilities. A large amount of CFD work has been done to validate existing and to find new loss functions but even more is required to cover all needed geometries and flow cases.

- Models for total pressure loss over fire. Currently this pressure loss is given as input. Fortunately, for most fire studies it is a negligible contribution to overall losses, but exceptions to this exist.
- Particle emission models need further improvement and validation.
- Wall film coefficients need further study under both low and unsteady velocity conditions.

6 CONCLUSION

A new simulation suite for rail and road ventilation and fire studies has been developed and validated. The new models enable study of a range of ventilation related phenomena that previously required application of several different tools and significant effort. Some effects such as combination of train and buoyancy forces, train particle emissions, dynamic road traffic and feedback control systems are, to the best of our knowledge, not treated in any available tunnel ventilation tool.

REFERENCES

(1) Subway Environmental Design Handbook Volume II: Subway Environment Simulation Computer Program (SES), Part 2, Programmer's Manual, 1980, Prepared for U.S. Department of Transportation

(2) Vardy A E. Thermotun/5.2, User Manual; Dundee Tunnel Research, August 2001

(3) Tiller, M., P.Bowles, H.Elmqvist, D.Brück, S. E.Mattson, A.Möller, H.Olsson and M.Otter 2000. Detailed Vehicle Powertrain Modeling in Modelica. Modelica Workshop 2000 Proceedings, pp.169-178

(4) Karlsson, H.L., Nilsson, L. and Möller, L. Subway particles are more genotoxic than street particles and induce oxidative stress in cultured human lung cells. Chem. Res. Toxicol., 18 (1), 19 -23, 2005

(5) P.Sahlin, P. Grozman, IDA Simulation Environment - a tool for Modelica based end-user application deployment, Proc. of the Third International Modelica Conference, Linköping, Sweden, Nov. 2003

(6) Incropera, F. P., DeWitt, D.P. (2002), "Fundamentals of Heat and Mass Transfer", 5th edition, John Wiley & Sons, Inc, p. 355, 492, 917, USA 2002

(7) Gardel, A. (1957), Les Pertes de Charge dans les Ecoulements au Travers de Branchements en Te, Bull. Tech. De la Suisse Romande, 83, 123-130, 144-148, 1957.